Nuclear forward glory, σ_R and f_N (0°) in the scattering of ^{6}He by carbon

A. N. Ostrowski,[1] A. C. Shotter,[1] W. Galster,[2] S. Cherubini,[2] T. Davinson,[1] A. M. Laird,[1] and A. Ninane[2]
[1]*Department of Physics and Astronomy, University of Edinburgh, Edinburgh EH9 3JZ, United Kingdom*
[2]*Département de Physique Nucléaire, Université Catholique, Louvain-la-Neuve, Belgium*
(Received 1 April 1999; published 9 November 1999)

Using the generalized optical theorem for charged particles, the total reaction cross section σ_R and the nuclear scattering amplitude f_N at 0° have been determined model independently for the first time in the ^{6}He+^{12}C system. A large fraction of σ_R is accounted for by $f_N(0°)$ — a manifestation of the nuclear forward glory effect. A comparison with the ^{6}Li+^{12}C system supports the prediction that the high break-up probability of ^{6}He reduces the fraction of the total reaction cross section accounted for by the nuclear scattering amplitude at 0°. [S0556-2813(99)03011-3]

PACS number(s): 25.60.Dz, 25.60.Bx, 25.60.Gc

I. INTRODUCTION

The nuclear forward glory effect, which is a result of the interference of the forward nuclear and Coulomb scattering amplitudes, has already been observed in a measurement [1] at nonvanishing Coulomb parameters η in the scattering of ^{12}C by carbon. It manifests itself in an enhancement of the nuclear scattering amplitude $f_N(0°)$, i.e $f_N(0°)$ accounts for a large part of the total reaction cross section σ_R. Both quantities can be determined by using the generalized optical theorem (GOT) for charged particles [2], which relates them model independently to elastic scattering angular distributions. The knowledge of $f_N(0°)$ and σ_R imposes additional restrictions on optical potentials describing the scattering in the system under investigation. In the present paper we report an experiment that applies the GOT to exotic nucleus scattering for the first time.

The interest in studying the ^{6}He nucleus is connected to the low binding energy of its *p*-shell neutrons, which leads to peculiarities in their density distribution. ^{6}He is regarded as the ''benchmark'' nucleus for the theoretical understanding of these features, since its tightly bound ^{4}He core makes it an ideal test case for the study of so-called ''Borromean'' neutron-rich three-body clusters [3].

In the present paper, we study whether the low neutron binding energy of only 975 keV for ^{6}He reduces the nuclear forward glory effect due to flux losses from the elastic channel related to its high break-up probability. To study the influence of neutron separation energy differences on the forward elastic scattering, one has to compare projectiles of the same mass multiplet incident on the same target. To avoid the complication of different projectile nuclear charges, we will compare the scattering of ^{6}He and ^{6}Li by carbon at the same Coulomb parameter η, using data previously published by Poling *et al.* [4]. The effects that arise from the small difference in mass of the two projectiles can be neglected. This comparison will allow us to show that the tail in the density distribution of the valence neutrons in ^{6}He not only enhances the total reaction cross section σ_R, but also reduces the fraction of σ_R that is accounted for by the forward nuclear scattering amplitude $f_N(0°)$.

No experimental data for ^{6}He on carbon, having both the necessary energy and angular resolution to detect this effect, have been published to date. However, the advent of post-accelerated nuclear beams at energies in the vicinity of the Coulomb barrier and with intensities greater than 10^6 ions/s at Louvain-la-Neuve, Belgium, provides the opportunity to study the scattering of ^{6}He in detail.

In the following, a measurement of the elastic scattering of ^{6}He by carbon, reaching into the forward glory angular domain, is described. The generalized optical theorem will then be used to determine σ_R and $f_N(0°)$ for both ^{6}He and ^{6}Li scattering by carbon. In addition, the result of an optical model fit to the scattering data will be used to determine the glory angular momentum, which will be compared to the grazing angular momentum obtained from the scattering data using a sharp cut-off model. Finally, the nuclear forward glories in both systems will be compared to see whether the low break-up threshold in ^{6}He with respect to ^{6}Li changes the magnitude of the effect.

II. EXPERIMENT

A post-accelerated secondary ^{6}He beam of 5.9 MeV and 3×10^6 ions/s was scattered on gold and carbon targets of 180 and 50 μg/cm^2, respectively. In addition, a carbon plus gold target of $20+20$ μg/cm^2 was used for normalization purposes. The energy resolution in the beam was 0.8% full width half maximum. The Coulomb parameter $\eta = Z_{\text{projectile}}Z_{\text{target}}e^2/(\hbar v)$ is 1.9. The beam showed less than 20 ppm contamination of ^{12}C ions, which had the same magnetic rigidity as the ^{6}He beam due to their 2^+ charge state. The reaction products were simultaneously measured in two LEDA-type silicon strip detector arrays covering two different angular ranges from 6 to 14 deg with an angular resolution of less than 0.5 deg and from 23 to 65 deg in the laboratory, respectively. The setup has been described elsewhere [6]. Both the energy and the time of flight with respect to the cyclotron frequency were recorded for each reaction product. The energy resolution was 60 keV and was mainly due to the longitudinal emittance of the beam. The timing resolution of 4 ns was sufficient to discriminate ^{6}He from other reaction products, in particular ^{4}He. This, in connection with the energy spectra, enabled us to identify the elastic scattering unambiguously. The beam quality has been monitored by

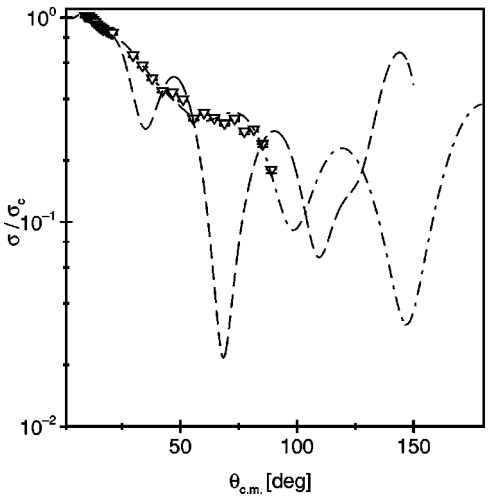

FIG. 1. Angular distribution of the measured differential elastic cross section normalized to the Coulomb cross section of ^{6}He $+^{12}$C at 5.9 MeV incident energy. Results of an optical model fit (dashed-dotted line) are also shown. The dashed line represents an angular distribution for the scattering of ^{6}Li$+^{12}$C 13 MeV incident energy (see text).

switching between the gold and the carbon target in short time steps. The solid angles have been calibrated using the scattering on the gold target, assuming pure Coulomb scattering.

Figure 1 shows the normalized angular distribution of the measured differential elastic cross section. The dashed-dotted line represents an optical model fit to the data. The optical model parameters are given in Table I. The dashed line shows the angular distribution for the scattering of ^{6}Li obtained using the phase shifts published in Ref. [4]. The Coulomb parameter values for the two different scattering systems differ only by 1%.

The quarter point angle obtained from the ^{6}He$+^{12}$C data set is 84 deg. Figure 1 shows that both scattering systems show considerable absorption already for angles less than 15 deg. The Coulomb rainbow at around 50 deg is more pronounced for the scattering of ^{6}Li. However, this is not entirely surprising, if the different Coulomb barrier heights are taken into account.

III. NUCLEAR FORWARD GLORY EFFECT AND THE GENERALIZED OPTICAL THEOREM

We recall that the nuclear forward glory effect manifests itself in heavy ion scattering in having moduli of the nuclear amplitude that follow a zero order Bessel function $J_0[l_g \sin(\Theta)]$ at forward angles Θ, where l_g denotes the glory angular momentum, which is essentially the grazing angular momentum [6,7]. Moreover, $|f_N(0°)|$ is largely enhanced, i.e., its value becomes comparable to the total reaction cross section σ_R divided by $4\pi/k$ [5].

TABLE I. Optical model parameters.

V_r	R_r	A_r	W_v	R_v	A_v	W_d	R_d	A_d
81.99	2.25	0.59	5.78	2.22	1.43	4.18	1.03	0.67

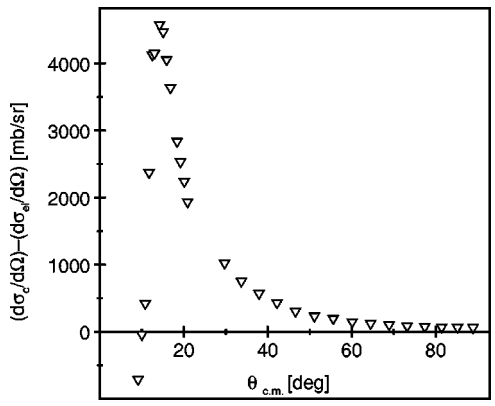

FIG. 2. Angular distribution of the differences of $[d\sigma/d\Omega(\theta)]_c$ and $[d\sigma/d\Omega(\theta)]_{\rm el}$ for ^{6}He$+^{12}$C at 5.9 MeV.

Hence, the magnitude of nuclear forward glory effect can be studied if σ_R and $|f_N(0°)|$ can be determined. Fortunately, the GOT relates σ_R and $|f_N(0°)|$ to elastic scattering angular distributions model independently via the sum-of-differences cross section $\sigma_{\rm SOD}(\Theta_0)$, which has been introduced by Holdeman and Thaler [8]:

$$\sigma_{\rm SOD}(\Theta_0) = 2\pi \int_{\Theta_0}^{\pi} \left\{ \left[\frac{d\sigma}{d\Omega}(\theta) \right]_c - \left[\frac{d\sigma}{d\Omega}(\theta) \right]_{\rm el} \right\} \sin\theta \, d\theta. \tag{1}$$

Here, $[d\sigma/d\Omega(\theta)]_c$ and $[d\sigma/d\Omega(\theta)]_{\rm el}$ denote the Coulomb and the differential elastic cross sections, respectively. A lower cut-off angle Θ_0 is introduced to cope with the divergence of the Coulomb cross section at 0°.

Since $\sigma_{\rm SOD}(\Theta_0)$ is the result of an integration over the angular range between Θ_0 and π, one might think that it is necessary to provide elastic angular distributions that reach well into the backward hemisphere. This would introduce huge experimental problems, even with stable beams. However, the differences in the integrand of Eq. (1) will become smaller and smaller with rising cut-off angle Θ_0. The upper limit for a particular difference is clearly given by the value attained by the Coulomb cross section alone.

Figure 2 shows the difference between $[d\sigma/d\Omega(\theta)]_c$ and $[d\sigma/d\Omega(\theta)]_{\rm el}$ for the measured data points. Figure 3 gives the result of the Holdeman-Thaler integral for the measured data points, given as triangles. The integration has been performed assuming that the differences for cutoff angles Θ_0 greater than the largest angle of the measured data are given by the Coulomb cross section. The error on the data points has been calculated following the procedure suggested by Marty [2]. Both the statistical error in the measured cross section and the precision in the determination of the scattering angle has been taken into account, as well as the approximation of the backward hemisphere differences by the Coulomb cross section. The error is dominated by the backward hemisphere approximation used. The error bars obtained in this way are smaller than the symbols shown in Fig. 3. The dashed dotted line shows the result of calculating $\sigma_{\rm SOD}(\Theta_0)$

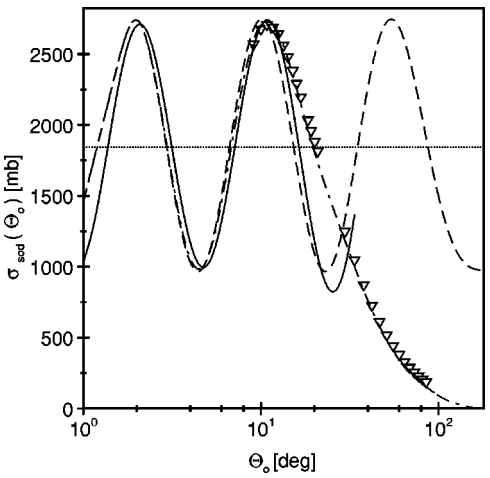

FIG. 3. Holdeman-Thaler integral for ^{6}He+^{12}C at 5.9 MeV (triangles), $\sigma_{\mathrm{SOD}}(\Theta_0)$ obtained using the optical model fit shown in Fig. 1 (dashed-dotted line), right-hand side of the GOT (dashed), and modified GOT fit to the maximum at 10.8 deg (see text). The dotted straight horizontal line represents the total reaction cross section value that has been determined using the GOT.

using the cross section derived from the optical model fit mentioned above. One can clearly see, that — as expected, due to the assumption of 100% absorption in the backward hemisphere — the measured data points lie slightly higher than the optical model data. However, at the maximum at 10.8 deg, the difference between the measured values and the optical model predictions is of the order of the experimental error bars. Hence, the error introduced by approximating the backward hemisphere absorption to be 100% is not prohibitive.

Equation (2) gives the generalized optical theorem (GOT) for charged particles [2]:

$$\sigma_{\mathrm{SOD}}(\Theta_0)=\sigma_R-\frac{4\pi}{k}|f_N(\Theta_0)|\sin\left\{\phi_N(\Theta_0)-2\sigma_0+2\eta\ln\left[\sin\left(\frac{\Theta_0}{2}\right)\right]\right\}+C(\Theta_0). \tag{2}$$

The GOT relates the sum-of-differences cross section $\sigma_{\mathrm{SOD}}(\Theta_0)$ to the total reaction cross section σ_R, the forward nuclear scattering amplitude $f_N(\Theta_0)$ in both modulus $|f_N(\Theta_0)|$ and phase ϕ_N, and a correction term $C(\Theta_0)$, that vanishes as Θ_0 goes to zero [2]. Here, σ_0 denotes the zero-order Coulomb phase.

For angles less than a certain angle Θ_g as defined in Eq. (3), the correction term $C(\Theta_0)$ in the GOT (2) becomes negligible [1]. Hence, $\sigma_{\mathrm{SOD}}(\Theta_0)$ starts to oscillate around σ_R for angles less than Θ_g with an amplitude that depends only on $|f_N(\Theta_0)|$. To identify for which angular range the correction term $C(\Theta_0)$ can be neglected, an angular distribution has been generated using the optical model fit to the measured data points, which has then in turn been used to calculate $\sigma_{\mathrm{SOD}}(\Theta_0)$ given by the dashed-dotted line in Fig. 3.

The dashed line in Fig. 3 shows the values attained by the right-hand side of the GOT neglecting the correction term

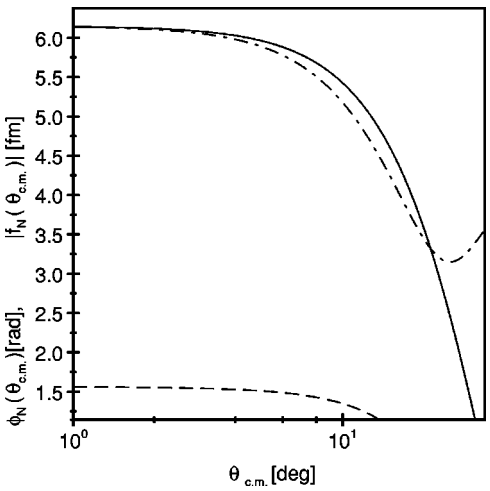

FIG. 4. Comparison of $|f_N(\Theta_{\mathrm{c.m.}})|$ obtained from the optical model fit (dashed-dotted line) and a zero order Bessel function fit following Eq. (4) given in fm (solid). The dashed line shows the phase of the nuclear scattering amplitude $\phi_N(\Theta_{CM})$ in radians.

$C(\Theta_0)$. Moreover, following Marty's approach [2], both $|f_N(\Theta_0)|$ and $\phi_N(\Theta_0)$ have been replaced by $|f_N(0°)|$ and $\phi_N(0°)$, respectively, which have been calculated using the optical model fit to the measured data points. In addition, the total reaction cross section σ_R used to calculate the dashed line is also taken from the optical model fit. Clearly for cut-off angles less than 10 deg this approximation falls almost on top of the optical model data generated $\sigma_{\mathrm{SOD}}(\Theta_0)$. Hence, for such angles the correction term $C(\Theta_0)$ can be neglected. This offers the possibility to deduce in a model-independent way σ_R, and the $|f_N(0°)|$ from elastic scattering data provided that the experiment yields angular distributions, which are reaching into the glory angular domain, i.e., for angles less than Θ_g. A limit on Θ_g can be deduced from the semi-classical scattering theory [7]:

$$\Theta_g=\frac{3\pi}{4l_g}. \tag{3}$$

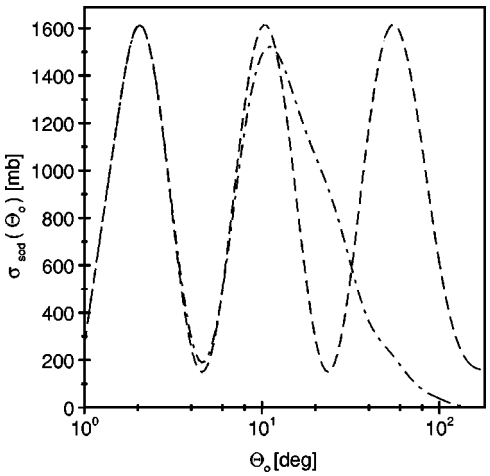

FIG. 5. $\sigma_{\mathrm{SOD}}(\Theta_0)$ for ^{6}Li+^{12}C at 13.0 MeV incident energy obtained using the phase shift analysis result shown in Fig. 1 (dashed-dotted line), right-hand side of the GOT (dashed line) (see text).

IV. DETERMINATION OF σ_R AND $|F_N(0°)|$

As can be seen from Fig. 3, the measured data points reach only just in the angular domain that is covered by the predictive power of the GOT neglecting the correction term $C(\Theta_0)$. As mentioned above, $|f_N(0°)|$ and $|f_N(\Theta_0)|$ are related by [5]

$$|f_N(\Theta_{\text{c.m.}})| = |f_N(0°)| \times J_0\{l_g \sin(\Theta_{\text{c.m.}})\} \tag{4}$$

in the glory angular domain. The dashed-dotted line in Fig. 4 shows the behavior of $|f_N(\Theta_{\text{c.m.}})|$ obtained from the optical model fit. The solid line shows the right-hand side of Eq. (4). However, the value attained by l_g of $4\hbar$ is twice the grazing angular momentum determined with the sharp cutoff model using the quarter point angle. In addition, Fig. 4 shows the behavior of the phase $\phi_N(\Theta_{\text{c.m.}})$ of the nuclear scattering amplitude.

The solid line in Fig. 3 shows the result of a fit using Eq. (2) to the maximum in the data points at 10.8 deg. It has been obtained using the GOT following Marty's approach [2], which allows the determination of σ_R and $|f_N(0°)|$. The correction term has been neglected. The way in which the fit parameters can be calculated is described in the following. At a maximum, the GOT simplifies to

$$\sigma_{\text{SOD}}(\Theta_{\max}) = \sigma_R + \frac{4\pi}{k}|f_N(\Theta_{\max})| + C(\Theta_{\max}). \tag{5}$$

The phase of the forward nuclear scattering amplitude is then given by

$$\phi_N(\Theta_{\max}) = \frac{3}{2}\pi + 2\sigma_0 - 2\eta \ln\left[\sin\left(\frac{\Theta_{\max}}{2}\right)\right]. \tag{6}$$

Using the next data point at a lower cut-off angle Θ_1 and applying the modified GOT, one finds

$$\sigma_{\text{SOD}}(\Theta_1) = \sigma_R - \frac{4\pi}{k}|f_N(\Theta_1)|\sin\left\{\phi_N(\Theta_1) - 2\sigma_0 + 2\eta \ln\left[\sin\left(\frac{\Theta_1}{2}\right)\right]\right\} + C(\Theta_1). \tag{7}$$

Neglecting the small changes in $|f_N|$ and ϕ_N going from $\Theta_{\max}$ to Θ_1 (cf. Fig. 4) and neglecting the differences in the correction terms $C(\Theta_{\max})$ and $C(\Theta_1)$, the subtraction of Eq. (7) from Eq. (5) then yields

$$\sigma_{\text{SOD}}(\Theta_{\max}) - \sigma_{\text{SOD}}(\Theta_1) \cong \frac{4\pi}{k}|f_N(\Theta_{\max})|\left\{1 + \sin\left[\phi_N(\Theta_{\max}) - 2\sigma_0 + 2\eta \ln\left\{\sin\left(\frac{\Theta_1}{2}\right)\right\}\right]\right\}. \tag{8}$$

Using Eq. (4) one finds $|f_N(0°)|$,

$$|f_N(0^o)| \cong \frac{k}{4\pi} \times \frac{\sigma_{\text{SOD}}(\Theta_{\max}) - \sigma_{\text{SOD}}(\Theta_1)}{J_0\{l_g \sin(\Theta_{\max})\} \times \left\{1 + \sin\left[\phi_N(\Theta_{\max}) - 2\sigma_0 + 2\eta \ln\left\{\sin\left(\frac{\Theta_1}{2}\right)\right\}\right]\right\}}. \tag{9}$$

This result and Eq. (4) can then be used to determine $|f_N(\Theta_{\max})|$ provided the correction term can be neglected. Thus, using Eq. (5), σ_R can be calculated from

$$\sigma_R \cong \sigma_{\text{SOD}}(\Theta_{\max}) - \frac{4\pi}{k}|f_N(\Theta_{\max})|. \tag{10}$$

In the following, Eq. (6) has been used to determine $\phi_N(\Theta_{\max})$. In addition, Eqs. (4) and (9) have been used to deduce $|f_N(\Theta_{\max})|$. The total reaction cross section σ_R has been inferred from Eq. (10).

The results of the fits to the maximum at $\Theta_{\max} = 10.8$ deg are as follows: (i) The phase of the nuclear scattering amplitude $\phi_N(\Theta_{\max})$: 1.30 rad ± 0.01 rad. (ii) The modulus of the nuclear scattering amplitude $|f_N(\Theta_{\max})|$: 5.10 fm ± 0.04 fm. (iii) The modulus of the nuclear scattering amplitude at 0 deg calculated using Eq. (4) and $l_g = 4\hbar$ $|f_N(0°)|$: 5.90 fm ± 0.04 fm. (iv) The total reaction cross section σ_R: 1840 mb ± 20 mb.

In Fig. 5 the dashed-dotted line shows $\sigma_{\text{SOD}}(\Theta_{\max})$ calculated using the phase shifts given in Ref. [4] for the scattering of ^{6}Li by carbon. Again the maximum at the largest cut-off angle has been used to fit σ_R and $|f_N(0°)|$. The results are (i) the modulus of the nuclear scattering amplitude at 0 deg calculated using Eq. (4) and $l_g = 4\hbar$ $|f_N(0°)|$: 7.5 fm; (ii) the total reaction cross section σ_R: 880 mb.

V. CONCLUSION

For the first time the nuclear forward glory effect has been observed in the scattering of the exotic nucleus ^{6}He by carbon, which manifests itself in a large value that is attained by the modulus of the nuclear scattering amplitude $|f_N|$ at 0 deg. To determine this quantity, a model-independent analysis based on the generalized optical theorem for charged particles has been performed, which was possible though no backward hemisphere data could be obtained in this radioactive nuclear beam based experiment.

A comparison between σ_R and $(4\pi/k)$ $|f_N(0°)|$ for the scattering of ^{6}He by carbon shows that the scattering amplitude at 0 deg accounts for almost 50% of the total reaction

cross section in the ^{6}He induced scattering. In the ^{6}Li case, however, almost 75% of σ_R is accounted for. This suggests that the low binding energy of the valence neutrons in ^{6}He leads to a reduced nuclear forward glory effect.

From our results we may conclude that the low breakup threshold in ^{6}He leads to a loss of flux from the elastic channel that reaches well into the glory angular domain, i.e., large impact parameters. This is also reflected in the total reaction cross section, which has been determined for the first time for ^{6}He$+^{12}$C. σ_R is twice as high as for ^{6}Li $+^{12}$C at the same Coulomb parameter value.

ACKNOWLEDGMENTS

The authors would like to thank A. di Pietro for support during the experiment and for a critical reading of the manuscript. Moreover, they wish to thank the staff at the Cyclotron Research Center accelerator facility in Louvain-la-Neuve, Belgium, for their effort in providing a good quality and intensity radioactive beam. This work was supported by the Engineering and Physical Sciences Research Council under Reference No. GR/M60095 and the European Commission by their ''Access to Large Scale Facility Program.''

[1] A.N. Ostrowski, W. Tiereth, D. Brandl, Z. Bazrak, and H. Voit, Phys. Lett. B **232**, 46 (1989); A.N. Ostrowski, W. Tiereth, and H. Voit, Phys. Rev. C **44**, 2082 (1991).

[2] C. Marty, Z. Phys. A **309**, 261 (1983); Z. Phys. A **322**, 499 (1985).

[3] B.V. Danilin, I.J. Thompson, J.S. Vaagen, and M.V. Zhukov, Nucl. Phys. **A632**, 383 (1998).

[4] J.E. Poling, E. Norbeck, and R.R. Carlson, Phys. Rev. C **5**, 1819 (1972).

[5] J. Barrette and N. Alamanos, Nucl. Phys. **A441**, 733 (1985); Phys. Lett. B **153**, 208 (1985).

[6] A.N. Ostrowski, A.C. Shotter, W. Bradfield-Smith, A.M. Laird, A. Di Pietro, T. Davinson, S. Morrow, P.J. Woods, S. Cherubini, W. Galster, J.S. Graulich, P. Leleux, L. Michel, A. Ninane, J. Vervier, M. Aliotta, C. Cali, F. Cappuzzello, A. Cunsolo, C. Spitaleri, J. Gorres, M. Wiescher, J. Rahighi, and J. Hinnefeld, J. Phys. G **24**, 1553 (1998).

[7] K.W. Ford and J.A. Wheeler, Ann. Phys. (N.Y.) **7**, 259 (1959).

[8] J.T. Holdemann and R.M. Thaler, Phys. Rev. **139**, B1186 (1965).